

Communication

Direct Interaction of Zirconia Nanoparticles with Human Immune Cells

Anna M. Barbasz *  and Barbara Dyba 

Department of Biochemistry and Biophysics, Institute of Biology and Earth Sciences, University of the National Education Commission, 30-084 Kraków, Poland

* Correspondence: anna.barbasz@up.krakow.pl

Abstract: Nanomaterials play a crucial role in various aspects of modern life. Zirconia nanoparticles, extensively employed in medicine for fortifying and stabilizing implants in reconstructive medicine, exhibit unique electrical, thermal, catalytic, sensory, optical, and mechanical properties. While these nanoparticles have shown antibacterial activity, they also exhibit cytotoxic effects on human cells. Our research focuses on understanding how the cells of the human immune system (both the innate response, namely HL-60 and U-937, and the acquired response, namely HUT-78 and COLO-720L) respond to the presence of zirconium (IV) oxide nanoparticles (ZrO₂-NPs). Viability tests indicate that ZrO₂-NPs exert the highest cytotoxicity on HL-60 > U-937 > HUT-78 > COLO 720L cell lines. Notably, concentrations exceeding 100 µg mL⁻¹ of ZrO₂-NPs result in significant cytotoxicity. These nanoparticles readily penetrate the cell membrane, causing mitochondrial damage, and their cytotoxicity is associated with heightened oxidative stress in cells. The use of ZrO₂-NP-based materials may pose a risk to immune system cells, the first responders to foreign entities in the body. Biofunctionalizing the surface of ZrO₂-NPs could serve as an effective strategy to mitigate cytotoxicity and introduce new properties for biomedical applications.

Keywords: cytotoxicity; acquired immunity; innate immunity; zirconium oxide nanoparticles



Citation: Barbasz, A.M.; Dyba, B. Direct Interaction of Zirconia Nanoparticles with Human Immune Cells. *Biophysica* **2024**, *4*, 83–91. <https://doi.org/10.3390/biophysica4010006>

Academic Editors: Marlene Lucio and Maciej Monedeiro-Milanowski

Received: 2 January 2024

Revised: 25 January 2024

Accepted: 9 February 2024

Published: 14 February 2024



Copyright: © 2024 by the authors. Licensee MDPI, Basel, Switzerland. This article is an open access article distributed under the terms and conditions of the Creative Commons Attribution (CC BY) license (<https://creativecommons.org/licenses/by/4.0/>).

1. Introduction

Any potentially antibacterial nanomaterial with bioactivity should undergo screening for nano-cytotoxicity to human cells. The widespread development and use of nanotechnologies in everyday life expose the human body to potential, often inadvertent, contact with them. As demonstrated by silver nanoparticles, a meticulous analysis of interactions with living cells yields a wealth of sometimes unsettling data. The observed antibacterial, antiviral, or anticancer activity often translates into cytotoxic effects against “normal” cells.

Zirconia (IV) oxide (zirconium), a material long utilized in medicine to fortify and stabilize implants in reconstructive medicine [1–4], has garnered attention. Zirconia oxide ceramic nanostructures have been employed as drug carriers as well [5,6]. At the nanoscale, the properties of a substance often undergo dramatic changes. Zirconia nanoparticles, known for their unique electrical, thermal, catalytic, sensory, optical, and mechanical properties [7–9], function as p-type semiconductors with piezoelectric properties. They find wide application in bone and dental implants, photocatalysis, fuel cells, and gas sensors [7,10–13].

As evident in the literature, zirconia nanoparticles are generally considered to have low toxicity. However, an increasing number of papers highlight dose-dependent toxicity, nanoparticle size, and incubation time as crucial factors. Antibacterial properties have been demonstrated against various microorganisms, including *Staphylococcus aureus*, *S. mutans*, *S. mitis*, *Escherichia coli*, *Salmonella typhi*, *Pseudomonas aeruginosa*, *Klebsiella oxytoca*, *Rothia mucilaginosa*, and *Rothia dentocariosa*, as well as the fungi *Candida albicans*, *Aspergillus niger*, *Rhizoctonia solani*, and *Pestalotiopsis versicolor* [14].

Preliminary studies on the impact of ZrO₂-NPs on cancer cells have also been conducted. These studies indicate that the presence of zirconia nanoparticles affects the viability of various cell lines, including human colon carcinoma (HCT-116), human lung carcinoma (A-549), human breast cancer MCF-7, HepG2, HeLa, human skin keratinocyte (HaCaT), and HT29 cells, as well as rat PC12 and mouse N2a cells [15–20]. However, the mechanism behind the cytotoxic effect on tumor cells remains incompletely understood. Reactive oxygen species (ROS) generated in the presence of ZrO₂-NPs appear to be the primary contributors. It is essential to note that the results obtained thus far are not directly comparable, due to the use of different types of nanoparticles, including variations in biofunctionalized forms.

The objective of our research is to investigate the response of human immune system cells to commercially available zirconium (IV) oxide nanoparticles (ZrO₂-NPs). For our study, we selected cell lines representing both the innate response (HL-60 and U-937) and the acquired response (HUT-78 and COLO-720L). Following the initial diagnosis, we conducted tests to identify the cytotoxic mechanisms of the chosen nanoparticles.

2. Materials and Methods

2.1. Nanoparticles

Commercially available (Sigma-Aldrich, St. Louis, MO, USA) zirconium (IV) oxide nanoparticles (ZrO₂-NPs) 10 wt% in H₂O were used. According to the information provided by the manufacturer, the nanoparticle's diameter was >100 nm (by the method of measuring the surface area of nanomaterials using the Brunauer–Emmett–Teller (BET) surface adsorption method) for water dispersion.

The particles were suspended in RPMI 1640 medium, supplemented with Pen-Strep without any FBS, to obtain a stock solution for biological experiments.

The average hydrodynamic diameter (calculated from diffusion coefficient) was 280.100 ± 8.954 , polydispersity index (PDI) was 0.186 ± 0.005 , zeta potential (ζ) was -24.800 ± 3.176 , and electrophoretic mobility (Mob) was -1.953 ± 0.261 of ZrO₂-NPs suspension (6.25 mg/L), which were determined by dynamic light scattering (DLS) using the Malvern Zetasizer Nano ZS (Malvern Analytical Ltd., Malvern, UK). Ultrapure water was used as a dispersant. Measurements were made at T = 25 °C.

2.2. Cell Cultures and Nanoparticle Treatment

COLO-720L, HUT-78, U-937, and HL-60 cell lines were received from the American Type Culture Collection (ATCC). The cells were cultured in RPMI 1640 medium containing 10% bovine serum (FBS) and 0.01% penicillin–streptomycin. The culture medium, antibiotics, and serum were purchased from CytoGen GmbH. Stock suspension of ZrO₂-NPs was diluted in RPMI 1640 medium to the required concentration.

2.3. Cell Viability Assay

The MTT tetrazolium salt colorimetric assay described by Mosmann (1983) [21] was used to detect the cytotoxicity of the ZrO₂-NPs. Cells were cultured in 96-well plates in an amount of 0.1×10^6 cell/well. After 24 or 48 h incubation with nanoparticles (final volume of suspension equal to 0.2 mL), 50 μ L MTT solution (of concentration 5 mg/mL) was added to each well and incubated for 2 h at 37 °C. Then, 0.4 mL of dimethyl sulfoxide (DMSO) was added and kept for 5 min. After centrifugation, the optical density of supernatant was read at 570 nm.

2.4. Membrane Damage Assay

The lactate dehydrogenase (LDH) assay was used to determine the damage of the membrane. Cells (in an amount of 0.1 million cells per well) were incubated in the presence of the nanoparticles for 48 h. One hundred microliters of supernatants was added to a mixture containing 10 μ L of 0.14mM NADH and 0.5 mL of 0.75mM mm sodium pyruvate. After incubation for 30 min at 37 °C, 0.5 mL of 2,4-dinitrophenylhydrazine was added to

the solution. After 1 h, the absorbance of the formed hydrazone was measured spectrophotometrically at 450 nm. The amount of LDH released after complete disruption of the cell membrane by sonification was taken as a control.

2.5. Nitric Oxide Production

Cells (in an amount of 0.2 million cells per well) were treated with ZrO₂-NPs. After a 48 h treatment, the supernatants were collected and centrifuged. Nitric oxide (NO) production was quantified spectrophotometrically using the Griess reagent (Sigma-Aldrich). The absorbance was measured at 540 nm, and the nitrite concentration was determined using calibration curve.

2.6. Determination of Lipid Peroxidation

Cells (in an amount of 0.2 million cells/well) treated with ZrO₂-NPs were collected and centrifuged after 48 h of contact. Cells' pellets were homogenized in 5 mL of 0.5% trichloroacetic acid (TCA). After centrifugation, 0.4 mL of supernatants were added to 1.25 mL of the mixture containing 10% TCA and 0.5% thiobarbituric acid (TBA). The mixture was boiled (30 min) in a dry thermoblock, then they were cooled down. The concentration of malondialdehyde (MDA) was determined spectrophotometrically at 532 nm using the molar extinction coefficient of MDA equal to 155 M⁻¹ cm⁻¹.

2.7. Determination of Caspase-9 (Casp-9)

Caspase-9 (casp-9) concentration in cell lysate was determined using the caspase-9 in vitro ELISA kit (Abcam, Cambridge, UK), according to the manufacturer's instructions. Cells were cultured in 48-well plates in an amount of 2 million cells per well at a final volume of 0.5 mL. After centrifugation, the pellet of cells was lysed by lysis buffer for 1 h. The standard or samples were inserting to wells, and then the rabbit detection antibody was added to each well. In the next step, after 2 h of incubation and washing, anti-rabbit-IgG antibody labeled with horseradish peroxidase (HRP) was added to wells. Samples were washed again and the color reaction was performed, after which the absorbance at 450 nm was measured and the concentration of caspase-9 samples was determined from calibration curve.

2.8. The Total Cell Resistance to Oxidation

The total cell resistance to oxidation (TRO) before and after treatment with the ZrO₂-NPs was tested by the modified spectrophotometric 2,2-diphenyl-1-picrylhydrazyl radical scavenging (DPPH) assay [22]. The cells were cultured in 24-well plates in an amount of 50 × 10³ cells per well in a volume of 0.5 mL per well. The pellets of cells, after centrifugation, were mixed with 0.2 mL of absolute methanol. The samples were vortexed for 1 min and then centrifuged (10 min, 10,000 × g). Next, 0.1 mL of supernatant and 0.2 mL of 0.125 mM DPPH on a 96-well plate were incubated for 30 min at room temperature in the dark. The absorbance of samples was measured at 517 nm using a microplate reader. Methanol was used as a control sample. The TRO of human cells, representing their ability to counteract an oxidation reaction, was calculated using the following formula:

$$\% \text{ inhibition} = 100 \frac{A_{\text{control}} - A_{\text{sample}}}{A_{\text{control}}}$$

2.9. Generation of Reactive Oxygen Species

Free radicals and other ROS were detected using a Cellular ROS/Superoxide Detection Assay Kit (Abcam, ab139476). In a 0.2-mL suspension, 10 × 10³ cells/mL were incubated with the ZrO₂-NPs and then with a ROS/Superoxide Detection Mix for 30 min at 37 °C. The positive control was incubated with 0.2 mmol/L pyocyanin. Then, the fluorescence intensities were measured at an emission wavelength of 520 nm (green) and 610 nm (orange; excitation wavelengths: 485 and 550 nm), respectively, using a Epoch BioTek Instruments microplate reader.

2.10. Statistical Analysis

Analyses were repeated five or three times and averaged (\pm SE). The significant differences compared with controls were estimated using the SAS ANOVA procedure. The statistical analysis was performed by Duncan's multiple range test, taking $p < 0.05$ using PC SAS 8.0. Statistical tests were carried out using STATISTICA 13.3. software.

3. Results

The metabolic activity of cells in the presence of selected nanoparticles is dose-dependent, as is the length of incubation with xenobiotics. Innate immunity cells (HL-60 and U-937) exhibit a more pronounced decrease in viability compared to acquired immunity cells (Figure 1A–D). Notably, promyelocyte cells (HL-60) display a 20% decrease in viability at a concentration of $100 \mu\text{g mL}^{-1}$ compared to the control, whereas promonocyte cells (U-937) show this decrease only at twice the concentration. The highest concentration of ZrO_2 -NPs used results in a 30% decrease in viability after 24 h and 45% after 48 h incubation with HL-60 cells. For U-937 cells, the viability decreases by 20% after 24 h and 45% after 48 h incubation, respectively. HUT-78 (T lymphocytes) lines and COLO-720L (B lymphocytes) at a concentration of $400 \mu\text{g mL}^{-1}$ ZrO_2 -NPs lose approximately 25% of their viability, compared to the control, after 48 h of incubation, with further prolongation to 72 h showing only a slight decrease in cell viability. Based on repeatable analyses, an incubation time of 48 h was chosen for further studies, focusing on HL-60 and HUT-78 cell lines as representative. Since screening studies indicated that low concentrations of ZrO_2 -NPs (in the range of 0 – $25 \mu\text{g mL}^{-1}$) do not significantly affect the tested cells, concentrations exceeding $25 \mu\text{g mL}^{-1}$ were examined. The study of cell membrane stability, measured as LDH leakage into the culture medium, revealed 1.5% more damage to the cell membrane in HUT-78 cells than in HL-60 cells (Figure 1E). Additionally, oxidative damage to the lipid bilayer was observed through the study of membrane lipid peroxidation (Figure 1F). At a concentration of $400 \mu\text{g mL}^{-1}$ ZrO_2 -NPs, the concentration of MDA increased more than twice compared to the control for both tested cell lines, with the HUT-78 line being more susceptible to lipid peroxidation. For HL-60 cells at a concentration of $400 \mu\text{g mL}^{-1}$ ZrO_2 -NPs, a more than two-fold increase in NO concentration was observed, compared to the control (Figure 2A). ZrO_2 -NPs also affected the activity of caspase-9, which activates the apoptotic pathway in cells. In both studies, cell lines at a concentration of $200 \mu\text{g mL}^{-1}$ exhibited three times higher levels of caspase-9, and at a concentration of $400 \mu\text{g mL}^{-1}$, four times higher than in the control (Figure 2B). The DPPH assay (measuring the total cell resistance to oxidation (TRO)) indicated an increase in the ability of cells to cope with an externally administered free radical (Figure 2C). Both cell lines showed a similar performance, with a 5-fold increase in % inhibition over the control. The generation of ROS as a result of exposure to ZrO_2 -NPs was demonstrated in Figure 2D, with both HL-60 and HUT-78 cells exhibiting a 5-fold (concentration $200 \mu\text{g mL}^{-1}$ ZrO_2 -NPs) and 7-fold (concentration $400 \mu\text{g mL}^{-1}$ ZrO_2 -NPs) increase in ROS production in the cells.

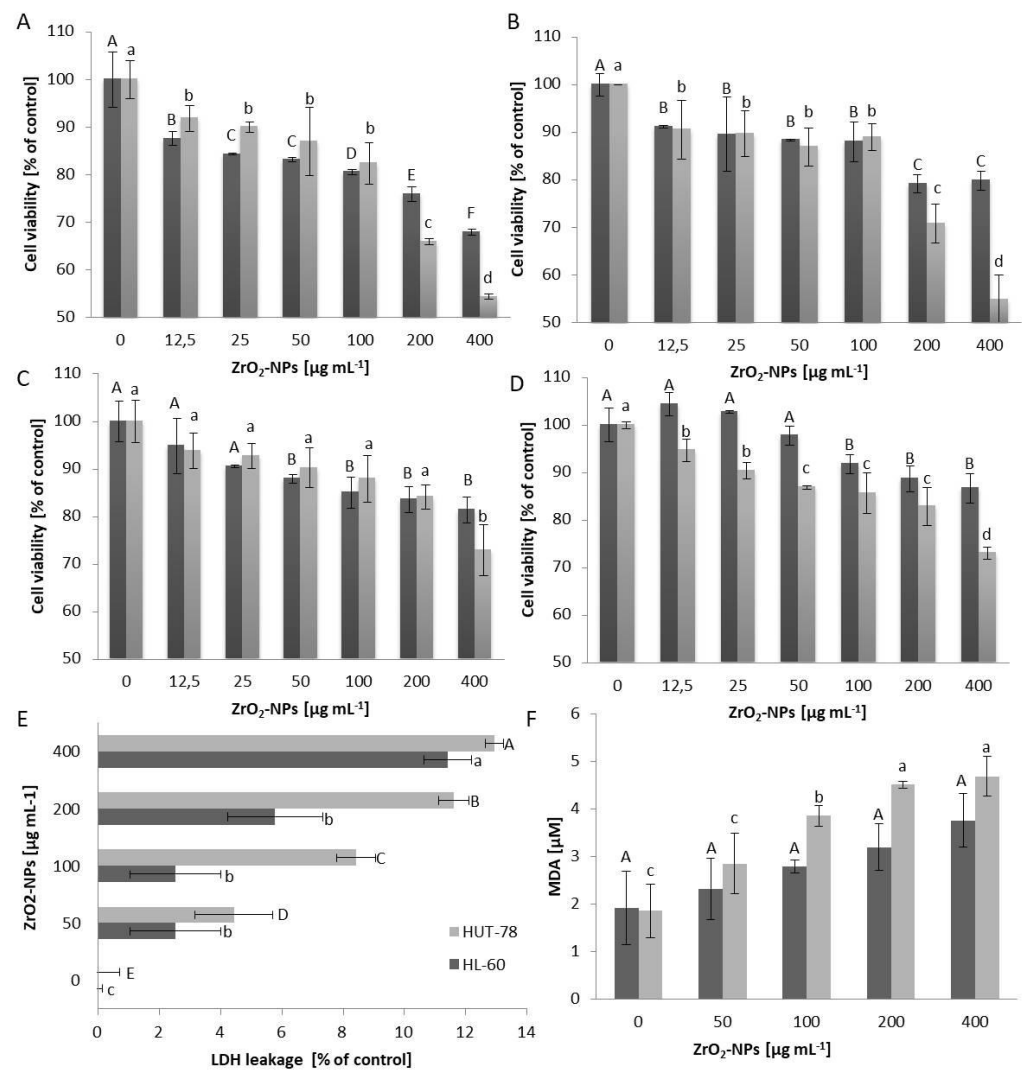


Figure 1. The viability (determined by MTT assays) of HL-60 (A), U-937 (B), HUT-78 (C), and COLO-720L (D) cells exposed for 24 h (dark bars) or 48 h (bright bars) to the action of zirconium (IV) oxide nanoparticles (ZrO₂-NPs), expressed as a percentage of the control group. The membrane damage determined via the lactate dehydrogenase leakage (LDH) (E) from HUT-78 and HL-60 after 48 h exposure to ZrO₂-NPs, compared with the control group. The extent of membrane lipid peroxidation in HUT-78 and HL-60 (F) cells, expressed as the MDA formation in response to 48 h ZrO₂-NPs treatment. Data points are means ± SD (five replicate trials). Different letters indicate significant ($p < 0.05$) differences between treatments.

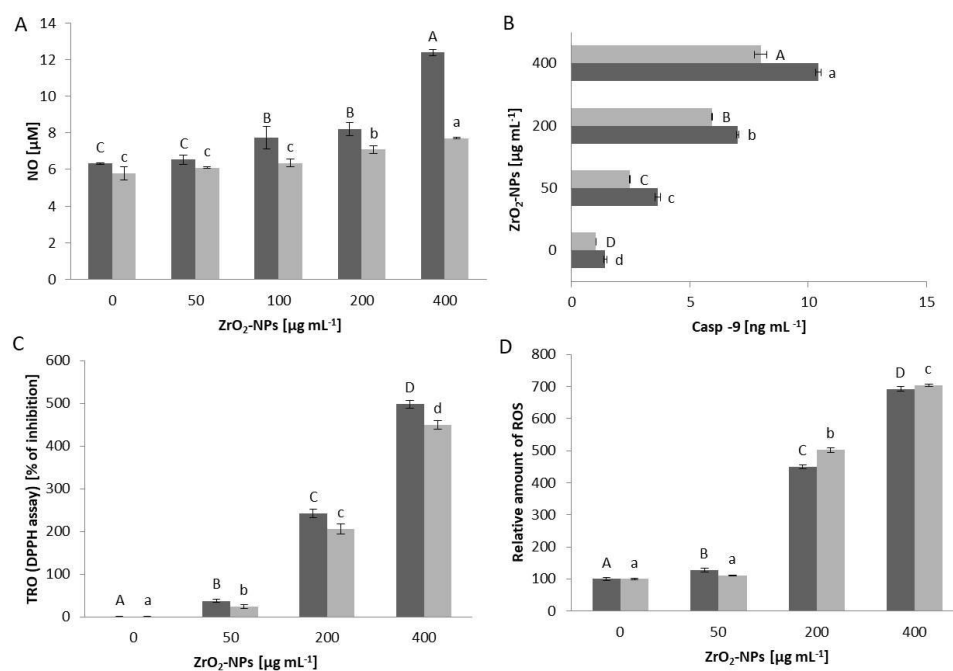


Figure 2. Relative (percentage of the control group) level of NO secreted by HUT-78 and HL-60 (A) cells after 48 h contact with ZrO₂-NPs. Concentration of caspase-9 (B) in the HUT-78 and HL-60 cell culture medium after 48 h treatment with ZrO₂-NPs. The TRO in systems containing HL-60 (dark bars) or HUT-78 (bright bars) cells (C). TRO was expressed as a percentage of reduction in DPPH level, in comparison to the control blank sample. There was a relative increase in the intracellular concentration of ROS in HL-60 (dark bars) or HUT-78 (bright bars) (D) cells after 48 h of treatment with ZrO₂-NPs. The ROS level was calculated as mean ± SD with the untreated control set to 100%. Data points are means ± SD (five replicate trials). Different letters indicate significant ($p < 0.05$) differences between treatments.

4. Discussion

Studies conducted on mice clearly indicated the acute toxicity of ZrO₂-NPs, as well as their biodistribution after intravenous administration into the body [23]. The authors demonstrated that doses in the range of 100–350 mg kg⁻¹ were safe for clinical use, but higher doses led to oxidative damage in liver tissue. This underscores the potential significant impact of nanomaterial-based implants on the body. ZrO₂-NPs released during oxidative dissolution can attain high local concentrations, significantly affecting body cells. Each implanted device elicits a response from the immune system cells, starting with innate and then acquired responses. Evaluating ZrO₂-NPs reactivity against model immune system cells can provide valuable insights.

ZrO₂-NPs in the cell culture medium exhibited a negative surface charge. The physicochemical properties of nanoparticles often play a crucial role in their interactions with cells. Interactions with proteins present in the environment remain a significant aspect. Among serum proteins, albumin is clearly the leader in the adsorption of metal oxide nanoparticles, including ZrO₂-NPs [24]. The toxic properties of ZrO₂-NPs may be related to the release of ionic zirconium from their surface as a result of oxidative dissolution processes [23,25]. On the other hand, it is known that the activity of metallic nanoparticles is also directly or indirectly modified by stabilizer molecules adsorbed on their surface, which, depending on their structure and properties, can mask or enhance the biological activity of nanoparticles. The influence of synthesis methods, reagents used, and purification methods, as shown by examining silver nanoparticles, can be crucial for enhancing or weakening the toxicity of nanomaterials [26,27].

Basic cell viability tests revealed distinct differences in cell sensitization to ZrO₂-NPs. Innate immunity cells (HL-60 and U-937) exhibited a greater decrease in viability compared to acquired immunity cells. Additionally, less differentiated cells (HL-60 promyelocytes) were more sensitive than more differentiated cells (U-937 promonocytes), consistent with findings related to silver nanoparticles [26]. This sensitivity is also time-dependent, indicating a higher susceptibility of cells derived from bone marrow, as confirmed in mouse bone marrow studies [28–30]. Lymphocyte interactions with metal and metal oxide nanoparticles reduced cell viability, associated with increased ROS concentration and the loss of mitochondrial function [31,32]. As demonstrated, ZrO₂-NPs reduce lymphocyte viability by an average of 20% at a concentration of 400 µg mL⁻¹ after 48 h of incubation, potentially modulating local inflammation.

Complementing viability tests, the cytoplasmic leakage test of lactate dehydrogenase (LDH) enzymes following cell membrane damage was conducted. Czyżowska et al.'s research [33] indicated that susceptibility to membrane damage correlated with the lipid composition of the membrane, observed in the determination of membrane lipid peroxidation. The loss of membrane integrity and higher peroxidation in membrane lipids indicated ROS-induced mechanisms in HUT-78 cells.

Could the cytotoxicity of ZrO₂-NPs be based on the same mechanism as for silver nanoparticles? Oxidative stress, reflected in increased ROS production, was observed in immune system representatives. The nearly seven-fold increase in ROS indicates substantial oxidative stress. However, after 48 h, cells gained the ability to remove ROS through enzymatic and non-enzymatic transformations, observed in the total cell resistance to oxidation (TRO) assessment. The TRO parameter, reflecting the system's oxidation resistance, increased with ZrO₂-NPs concentration. Contact with ZrO₂-NPs also exhibited an immune-stimulating effect on HL-60 cells and a pro-apoptotic effect on HL-60 and HUT-78 cells.

The latest research indicates that ZrO₂-NPs induces oxidative stress in animal cells, leading to oxidative damage not only in cellular proteins or lipids but also in genetic material. In detailed studies, Mourya et al. [34] demonstrated on V79 hamster cells that concentrations above 100 µg/mL result in significant DNA strand breaks. Increased DNA fragmentation was also observed after treating cells with PC12 and N2a [20]. ZrO₂-NPs also induce HeLa cell death through ROS-mediated mitochondrial apoptosis and autophagy [35]. Another study indicated that ZrO₂-NPs do not have a genotoxic effect on human peripheral blood lymphocytes and cultured human embryonic kidney cells [36,37]. Detailed research is still necessary, regarding the genotoxicity of ZrO₂-NPs towards cells of the human immune system.

In conclusion, ZrO₂-NPs are significantly cytotoxic at concentrations above 100 µg mL⁻¹, penetrating the cell membrane and damaging mitochondria. Their cytotoxicity correlates with high oxidative stress, resembling silver nanoparticles. The safety of ZrO₂-NP-based materials in relation to immune system cell damage. The surface biofunctionalization of ZrO₂-NPs may be an effective strategy to limit cytotoxicity and impart new properties for biomedical applications. Exposing a living organism to ZrO₂-NPs, as our research has shown, is associated with the risk of triggering an inflammatory response through various mechanisms. After all, the cells of the immune system are tasked with defending us against all xenobiotics, including those used for medical reasons.

Author Contributions: Conceptualization, A.M.B.; methodology, A.M.B.; software, A.M.B. and B.D.; validation, A.M.B. and B.D.; formal analysis, A.M.B.; investigation, A.M.B. and B.D.; resources, A.M.B.; data curation, A.M.B.; writing—original draft preparation, A.M.B.; writing—review and editing, A.M.B. and B.D.; visualization, A.M.B.; supervision, A.M.B. and B.D.; project administration, A.M.B.; funding acquisition, A.M.B. All authors have read and agreed to the published version of the manuscript.

Funding: This research received no external funding.

Data Availability Statement: Dataset available on request from the authors.

Conflicts of Interest: The authors declare no conflict of interest.

References

1. Comisso, I.; Arias-Herrera, S.; Gupta, S. Zirconium dioxide implants as an alternative to titanium: A systematic review. *J. Clin. Exp. Dent.* **2021**, *13*, e511–e519. [[CrossRef](#)]
2. Pieralli, S.; Kohal, R.-J.; Hernandez, E.L.; Doerken, S.; Spies, B.C. Osseointegration of zirconia dental implants in animal investigations: A systematic review and meta-analysis. *Dent. Mater.* **2018**, *34*, 171–182. [[CrossRef](#)]
3. Özkurt, Z.; Kazazoglu, E. Zirconia Dental Implants: A Literature Review. *J. Oral Implantol.* **2011**, *37*, 367–376. [[CrossRef](#)] [[PubMed](#)]
4. Apratim, A.; Eachempati, P.; Salian, K.K.; Singh, V.; Chhabra, S.; Shah, S. Zirconia in dental implantology: A review. *J. Int. Soc. Prev. Community Dent.* **2015**, *5*, 147–156. [[CrossRef](#)] [[PubMed](#)]
5. Nakarani, M.; Misra, A.K.; Patel, J.K.; Vaghani, S.S. Itraconazole nanosuspension for oral delivery: Formulation, characterization and in vitro comparison with marketed formulation. *Daru J. Fac. Pharm. Tehran Univ. Med. Sci.* **2010**, *18*, 84–90.
6. Tan, K.; Cheang, P.; Ho, I.A.W.; Lam, P.Y.P.; Hui, K.M. Nanosized bioceramic particles could function as efficient gene delivery vehicles with target specificity for the spleen. *Gene Ther.* **2007**, *14*, 828–835. [[CrossRef](#)] [[PubMed](#)]
7. Shinde, H.M.; Bhosale, T.T.; Gavade, N.L.; Babar, S.B.; Kamble, R.J.; Shirke, B.S.; Garadkar, K.M. Biosynthesis of ZrO₂ nanoparticles from *Ficus benghalensis* leaf extract for photocatalytic activity. *J. Mater. Sci. Mater. Electron.* **2018**, *29*, 14055–14064. [[CrossRef](#)]
8. Bansal, P.; Bhanjana, G.; Prabhakar, N.; Dhau, J.S.; Chaudhary, G.R. Electrochemical sensor based on ZrO₂ NPs/Au electrode sensing layer for monitoring hydrazine and catechol in real water samples. *J. Mol. Liq.* **2017**, *248*, 651–657. [[CrossRef](#)]
9. Mallakpour, S.; Ezhieh, A.N. Polymer Nanocomposites based on Modified ZrO₂ NPs and Poly(vinyl alcohol)/Poly(vinyl pyrrolidone) Blend: Optical, Morphological, and Thermal Properties. *Polym. Technol. Eng.* **2016**, *56*, 1136–1145. [[CrossRef](#)]
10. Gillani, R.; Ercan, B.; Qiao, A.; Webster, T.J. Nanofunctionalized zirconia and barium sulfate particles as bone cement additives. *Int. J. Nanomed.* **2009**, *5*, 1–11. [[CrossRef](#)]
11. Zhang, H.; Lu, H.; Zhu, Y.; Li, F.; Duan, R.; Zhang, M.; Wang, X. Preparations and characterizations of new mesoporous ZrO₂ and Y₂O₃-stabilized ZrO₂ spherical powders. *Powder Technol.* **2012**, *227*, 9–16. [[CrossRef](#)]
12. Shim, J.H.; Chao, C.-C.; Huang, H.; Prinz, F.B. Atomic Layer Deposition of Yttria-Stabilized Zirconia for Solid Oxide Fuel Cells. *Chem. Mater.* **2007**, *19*, 3850–3854. [[CrossRef](#)]
13. Ramamoorthy, R.; Dutta, P.K.; Akbar, S.A. Oxygen sensors: Materials, methods, designs and applications. *J. Mater. Sci.* **2003**, *38*, 4271–4282. [[CrossRef](#)]
14. Kumari, N.; Sareen, S.; Verma, M.; Sharma, S.; Sharma, A.; Sohal, H.S.; Mehta, S.K.; Park, J.; Mutreja, V. Zirconia-based nanomaterials: Recent developments in synthesis and applications. *Nanoscale Adv.* **2022**, *4*, 4210–4236. [[CrossRef](#)] [[PubMed](#)]
15. Saraswathi, V.S.; Santhakumar, K. Photocatalytic activity against azo dye and cytotoxicity on MCF-7 cell lines of zirconium oxide nanoparticle mediated using leaves of *Lagerstroemia speciosa*. *J. Photochem. Photobiol. B Biol.* **2017**, *169*, 47–55. [[CrossRef](#)] [[PubMed](#)]
16. Balaji, S.; Mandal, B.K.; Ranjan, S.; Dasgupta, N.; Chidambaram, R. Nano-zirconia—Evaluation of its antioxidant and anticancer activity. *J. Photochem. Photobiol. B Biol.* **2017**, *170*, 125–133. [[CrossRef](#)] [[PubMed](#)]
17. Chen, L.; Zhong, H.; Qi, X.; Shao, H.; Xu, K. Modified core-shell magnetic mesoporous zirconia nanoparticles formed through a facile “outside-to-inside” way for CT/MRI dual-modal imaging and magnetic targeting cancer chemotherapy. *RSC Adv.* **2019**, *9*, 13220–13233. [[CrossRef](#)] [[PubMed](#)]
18. Han, C.; Yang, J.; Gu, J. Immobilization of silver nanoparticles in Zr-based MOFs: Induction of apoptosis in cancer cells. *J. Nanoparticle Res.* **2018**, *20*, 77. [[CrossRef](#)]
19. Alzahrani, F.M.; Katubi, K.M.S.; Ali, D.; Alarifi, S. Apoptotic and DNA-damaging effects of yttria-stabilized zirconia nanoparticles on human skin epithelial cells. *Int. J. Nanomed.* **2019**, *14*, 7003–7016. [[CrossRef](#)]
20. Asadpour, E.; Sadeghnia, H.R.; Ghorbani, A.; Sedaghat, M.; Boroushaki, M.T. Oxidative stress-mediated cytotoxicity of zirconia nanoparticles on PC12 and N2a cells. *J. Nanoparticle Res.* **2016**, *18*, 14. [[CrossRef](#)]
21. Mosmann, T. Rapid colorimetric assay for cellular growth and survival: application to proliferation and cytotoxicity assays. *J. Immunol. Methods* **1983**, *65*, 55–63. [[CrossRef](#)]
22. Blois, M.S. Antioxidant determinations by the use of a stable free radical. *Nature* **1958**, *181*, 1199–1200. [[CrossRef](#)]
23. Yang, Y.; Bao, H.; Chai, Q.; Wang, Z.; Sun, Z.; Fu, C.; Liu, Z.; Liu, Z.; Meng, X.; Liu, T. Toxicity, biodistribution and oxidative damage caused by zirconia nanoparticles after intravenous injection. *Int. J. Nanomed.* **2019**, *14*, 5175–5186. [[CrossRef](#)] [[PubMed](#)]
24. Bozgeyik, K.; Kopac, T. Adsorption of Bovine Serum Albumin onto Metal Oxides: Adsorption Equilibrium and Kinetics onto Alumina and Zirconia. *Int. J. Chem. React. Eng.* **2010**, *8*. [[CrossRef](#)]
25. Hao, L.; Zhou, X.; Liu, J. Release of ZrO₂ nanoparticles from ZrO₂/Polymer nanocomposite in wastewater treatment processes. *J. Environ. Sci.* **2020**, *91*, 85–91. [[CrossRef](#)] [[PubMed](#)]
26. Barbasz, A.; Oćwieja, M.; Walas, S. Toxicological effects of three types of silver nanoparticles and their salt precursors acting on human U-937 and HL-60 cells. *Toxicol. Mech. Methods* **2016**, *27*, 58–71. [[CrossRef](#)] [[PubMed](#)]
27. Oćwieja, M.; Barbasz, A.; Walas, S.; Roman, M.; Paluszkiwicz, C. Physicochemical properties and cytotoxicity of cysteine-functionalized silver nanoparticles. *Colloids Surf. B Biointerfaces* **2017**, *160*, 429–437. [[CrossRef](#)] [[PubMed](#)]
28. Paik, S.-Y.R.; Kim, J.-S.; Shin, S.J.; Ko, S. Characterization, Quantification, and Determination of the Toxicity of Iron Oxide Nanoparticles to the Bone Marrow Cells. *Int. J. Mol. Sci.* **2015**, *16*, 22243–22257. [[CrossRef](#)] [[PubMed](#)]

29. Castro-Gamboa, S.; Garcia-Garcia, M.R.; Piñon-Zarate, G.; Rojas-Lemus, M.; Jarquin-Yañez, K.; Herrera-Enriquez, M.A.; Fortoul, T.I.; Toledano-Magaña, Y.; Garcia-Iglesias, T.; Pestryakov, A.; et al. Toxicity of silver nanoparticles in mouse bone marrow-derived dendritic cells: Implications for phenotype. *J. Immunotoxicol.* **2019**, *16*, 54–62. [[CrossRef](#)]
30. Alghriany, A.A.I.; Omar, H.E.-D.M.; Mahmoud, A.M.; Atia, M.M. Assessment of the Toxicity of Aluminum Oxide and Its Nanoparticles in the Bone Marrow and Liver of Male Mice: Ameliorative Efficacy of Curcumin Nanoparticles. *ACS Omega* **2022**, *7*, 13841–13852. [[CrossRef](#)]
31. Assadian, E.; Zarei, M.H.; Gilani, A.G.; Farshin, M.; Degampanah, H.; Pourahmad, J. Toxicity of Copper Oxide (CuO) Nanoparticles on Human Blood Lymphocytes. *Biol. Trace Element Res.* **2017**, *184*, 350–357. [[CrossRef](#)]
32. Prasad, K.S.; Selvaraj, K. Biogenic Synthesis of Selenium Nanoparticles and Their Effect on as(III)-Induced Toxicity on Human Lymphocytes. *Biol. Trace Element Res.* **2014**, *157*, 275–283. [[CrossRef](#)]
33. Czyżowska, A.; Dyba, B.; Rudolphi-Szydło, E.; Barbasz, A. Structural and biochemical modifications of model and native membranes of human immune cells in response to the action of zinc oxide nanoparticles. *J. Appl. Toxicol.* **2020**, *41*, 458–469. [[CrossRef](#)]
34. Mourya, D.; Dubey, K.; Jha, S.; Maurya, R.; Pandey, A.K. In Vitro Effects of Zirconia Nanoparticles: Uptake, Genotoxicity, and Mutagenicity in V-79 cells. *Biol. Trace Element Res.* **2023**, *202*, 927–940. [[CrossRef](#)]
35. Shang, Y.; Wang, Q.; Li, J.; Liu, H.; Zhao, Q.; Huang, X.; Dong, H.; Chen, W.; Gui, R.; Nie, X. Zirconia Nanoparticles Induce HeLa Cell Death through Mitochondrial Apoptosis and Autophagy Pathways Mediated by ROS. *Front. Chem.* **2021**, *9*, 522708. [[CrossRef](#)]
36. Demir, E.; Burgucu, D.; Turna, F.; Aksakal, S.; Kaya, B. Determination of TiO₂, ZrO₂, and Al₂O₃ Nanoparticles on Genotoxic Responses in Human Peripheral Blood Lymphocytes and Cultured Embryonic Kidney Cells. *J. Toxicol. Environ. Heal. Part A* **2013**, *76*, 990–1002. [[CrossRef](#)]
37. Di Virgilio, A.; Arnal, P.; Maisuls, I. Biocompatibility of core@shell particles: Cytotoxicity and genotoxicity in human osteosarcoma cells of colloidal silica spheres coated with crystalline or amorphous zirconia. *Mutat. Res. Toxicol. Environ. Mutagen.* **2014**, *770*, 85–94. [[CrossRef](#)] [[PubMed](#)]

Disclaimer/Publisher’s Note: The statements, opinions and data contained in all publications are solely those of the individual author(s) and contributor(s) and not of MDPI and/or the editor(s). MDPI and/or the editor(s) disclaim responsibility for any injury to people or property resulting from any ideas, methods, instructions or products referred to in the content.